ChemComm

Exploration of flow reaction conditions using machine-learning for enantioselective organocatalyzed Rauhut-Currier and [3+2] annulation sequence

Journal:	*ChemComm*
Manuscript ID	CC-COM-11-2019-008526.R1
Article Type:	Communication

COMMUNICATION

Exploration of flow reaction conditions using machine-learning for enantioselective organocatalyzed Rauhut-Currier and [3+2] annulation sequence

Received 00th January 20xx,
Accepted 00th January 20xx

DOI: 10.1039/x0xx00000x

Masaru Kondo[a], H.D.P. Wathsala[a], Makoto Sako[a], Yutaro Hanatani[a], Kazunori Ishikawa[b], Satoshi Hara[b], Takayuki Takaai[b], Takashi Washio*[b,c], Shinobu Takizawa*[a,c], Hiroaki Sasai*[a]

A highly atom-economical enantioselective organocatalyzed Rauhut-Currier and [3+2] annulation sequence has been established by using flow system. The suitable flow conditions were explored through reaction screening of multiple parameters using machine learning. Eventually, functionalized chiral spirooxindole analogues were obtained in high yield with good ee as a single diastereomer within one minute.

In the field of organic chemistry, the optimization of conditions is a crucial and unavoidable process in the development of a synthetic reaction in both academic and industrial research. The conventional procedure is to vary the reaction parameters individually while keeping the others constant (Fig. 1a). Therefore, an efficient and rapid reaction screening strategy is of significant interest to the scientific community. Machine-Learning (ML) is a robust and reliable tool that can be used to achieve efficient optimization.[1] Over the past decade, ML has been applied to various chemical fields such as drug discovery,[2] synthesis planning,[3] and material and catalyst design.[4] More recently, outstanding results with automated[5] and computational optimization procedures[6] have been reported. In theoretical and physical chemistry, Gaussian process regression (GPR),[7] which is a kernel-based statistical learning algorithm, has been increasingly applied to predict a variety of chemical properties as a black-box estimator under a given up to date dataset. Since it is difficult for chemists to understand the unclear tendency and correlation of each parameter of a novel reaction and its outcome without performing a thorough reaction optimization, GPR could be helpful in estimating the optimal conditions from experimental results by using a kernel-based method and conducting the minimum number of reactions for multi-parameter screening (e.g. flow reaction and electrolysis). (Fig. 1b).

Spirooxindole motifs are found in numerous natural products and biologically active molecules such as horsfiline, gelsemine, and marcfortine B.[8] To date, spirooxindole derivatives have attracted much attention in the area of antiviral drug discovery and development, owing to the high number of positive hits achieved by this scaffold.[8d-f] Although significant progress has been made in the

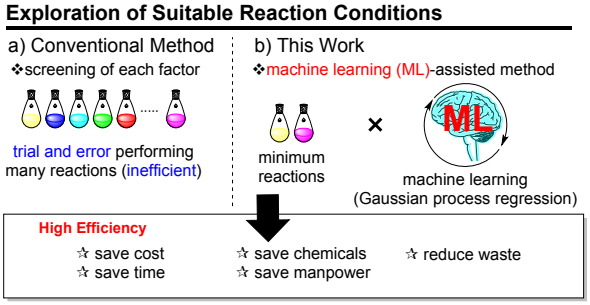

Fig. 1 Exploration of suitable reaction conditions through minimum experimental data with machine learning.

strategies capable of constructing multiple chiral centers are still in high demand.[8a-c,9] As part of our exploration of enantioselective domino processes with a single operation,[10] we were interested in developing the organocatalyzed Rauhut-Currier (RC) and [3+2] annulation sequence[11] of dienone **1** with allenoate **2** to access the highly functionalized chiral spirooxindole analogue **4**, bearing three contiguous chiral centers. The domino reaction of **1a** and **2a** as prototypical substrates in the presence of chiral organocatalyst **5** (20 mol %) was initially attempted in a batch process (Table 1). Among the organocatalysts examined, (*S*)-valine-derived catalyst **5a** bearing diphenylphosphine and benzoyl units promoted the desired domino reaction to afford spiro heterocycle **4a** with high regio- and stereoselectivity, albeit in 42% yield. In 2017, we and Huang independently reported highly active organocatalyst for the enantioselective intramolecular RC reaction of **1**,[10c,11d] however, neither amine catalyst **5e** nor Huang Cat. for the RC showed attractive outcomes on our desired domino reaction. Many unidentified products were also formed due to side reactions of dienone **1a** with the highly reactive intermediary RC product **3a**,[10c] and allenoate **2a** in the presence of catalysts **5**. In terms of enantioselectivity, the use of catalyst **5a** in toluene gave **4a** in 92% ee as a single diastereomer, but no significant improvement in the chemical yield of **4a** was accomplished in the batch system (see Supplementary Table S1, S2).

When we considered the reaction processes, we found that a micro-mixing flow system[12] offered a means of improving the chemical yield of product **4a** by suppressing undesired side reactions. Under rapid mixing with a micro mixer: Comet X-01[13] at dilute concentration of a mixture of substrates **1a** and **2a**, and catalyst **5a** (0.01 M for **1a** in toluene), the intramolecular RC reaction initially proceeded to afford

[a] *The Institute of Scientific and Industrial Research (ISIR), Osaka University, Mihogaoka, Ibaraki, Osaka 567-0047, Japan*
E-mail: taki@sanken.osaka-u.ac.jp, sasai@sanken.osaka-u.ac.jp
[b] *Department of Reasoning for Intelligence, ISIR, Osaka University,*
E-mail: washio@ar.sanken.osaka-u.ac.jp
[c] *Artificial Intelligence Research Center, ISIR, Osaka University*
Electronic Supplementary Information (ESI) available: See DOI: 10.1039/x0xx00000x

Table 1. Catalyst screening in batch system

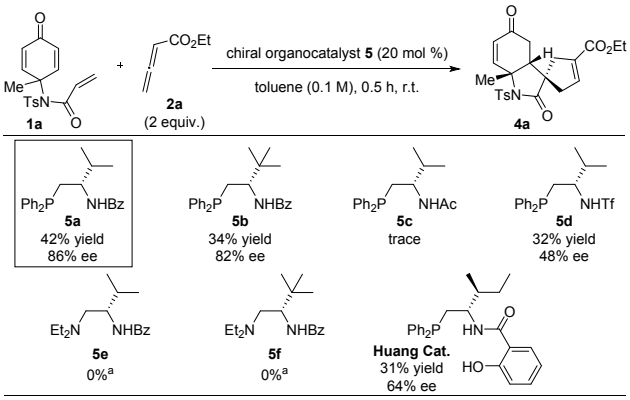

Reaction conditions: **1a** (0.03 mmol), **2a** (0.06 mmol), and catalyst (*S*)-**5** (20 mol%), in dry toluene. Yields were estimated by ^{1}H NMR using 1,3,5-trimethoxybenzene as an internal standard. Ees were determined by HPLC analysis (Daicel Chiralpak ID). [a] RC product **3a** was only observed.

the highly reactive dienone RC product **3a**, followed by intermolecular [3+2] annulation, leading to **4a** in 49% NMR yield (Table 2, entry 1).[14] This improved outcome prompted us to optimize reaction conditions in the flow system. Moreover, GPR on GPy, which is a programming library for Gaussian processes regression,[15] constructs a regression model by using a limited number of observed data through ML, and searches a subsequent appropriate parameter value by using the model as a surrogate model of the flow reaction conditions. To achieve the ML estimation of the suitable flow reaction conditions, the temperature (60–100 °C) and flow rate (1.0–3.0 mL/min) were first screened using GPy while maintaining the quantity of **2a** at 2.0 equiv. to minimize the cost of chemicals (entries 1–5) (see Supplementary Table S3 and Fig. S3)[16] with referencing the batch optimization outcomes. Standardization was performed to compensate for the large difference in scale between temperature and flow rate. Evaluation of the observed results using GPR illustrated the estimated yield from screening results of flow rate and temperature as shown in Fig. 2A (intense yellow: higher yield; intense black: lower yield).

This outcome encouraged us to focus on the yellow area in Fig. 2A predicting the optimal conditions. The confidence bounds (light blue area) in Fig. 2B and 2C indicated the flow rate and temperature that should be used to conduct the next experiments. The optimal flow rate and temperature were estimated to be 1.7 mL/min and 77 °C from the expected maximum value of the upper confidence bounds in Fig. 2B and 2C (red line). Secondly, the yield through screening of temperature (60–100 °C) and quantity of **2a** (1.0–4.0 equiv.) was estimated from Table 2 (entries 6–10) using a fixed flow rate of 1.7 mL/min as shown in Fig. 2D, Fig. 2E, and 2F (see Supplementary Table S4 and Fig. S4) show the next evaluations of temperature and the amount of **2a** obtained from the yellow ring in Fig. 2D. On the basis of Fig. 2E and 2F, the ML predicted reaction conditions were 2.0 equiv. of **2a** with a reaction temperature below 90 °C. Our ML-assisted exploring methodology of reaction conditions could narrow down multi-parameters more efficiently in comparison of the conventional trial and error screening. Considering all the results estimated by GPR and the experimental data in batch system, we decided the suitable flow reaction conditions as 2.0 equiv. of **2a** and a flow rate of 1.7 mL/min at 80 °C. In fact, when we applied the reaction conditions to a practical reaction, **4a** was isolated in 76% yield and 94% ee (Table 2, entry 11).[17]

Having the estimated optimal conditions, we investigated the substrate scope of the domino reaction (Scheme 1). Compounds **1b** (R^1 = Et) and **1c** (R^1 = ^{i}Pr) with aliphatic substituents afforded products

Table 2. Exploration of suitable reaction conditions[a]

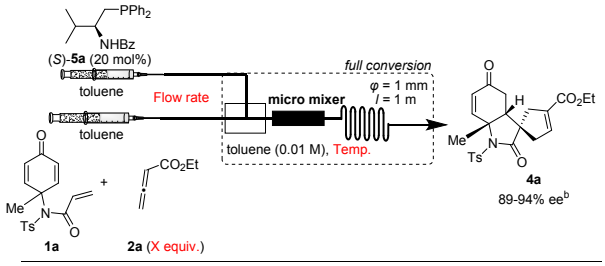

Entry	Flow rate (mL/min)	Temp. (°C)	**2a** (equiv.)	NMR yield[c] (%)
1	1.0	90	2.0	49
2	1.5	80	2.0	72
3	2.0	70	2.0	58
4	2.5	60	2.0	55
5	3.0	100	2.0	43
6	1.7	80	1.0	45
7	1.7	100	1.5	51
8	1.7	90	2.0	58
9	1.7	70	3.0	50
10	1.7	60	4.0	48
11[d]	1.7	80	2.0	78 (76)[e]

[a]Reaction conditions: **1a** (0.03 mmol), **2a** and catalyst (*S*)-**5a** (20 mol%), in degassed dry toluene (3 mL), micro mixer: Comet X-01, stainless-steel tube (internal diameter: 1.0 mm, length: 1.0 m) [b]Enantiomeric excess was determined by HPLC analysis (Daicel Chiralpak ID). [c]1,3,5-Trimethoxybenzene was used as an internal standard. [d]**4a** was obtained in 94% ee. [e]Isolated yield.

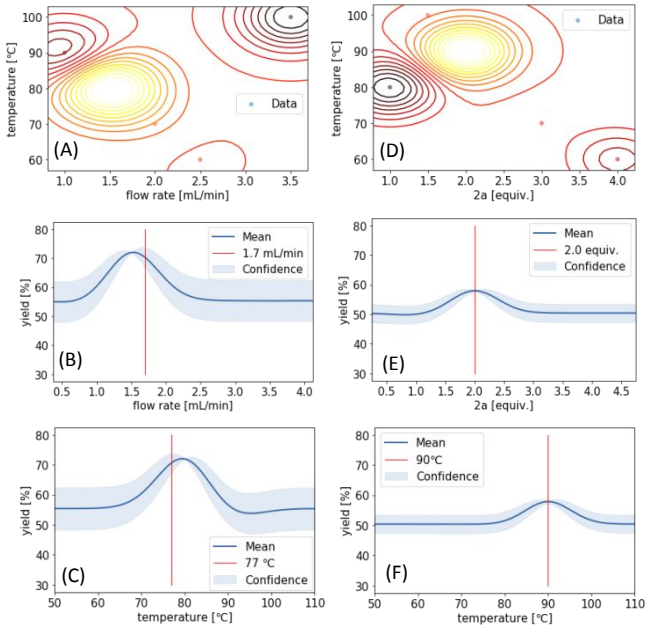

Fig. 2 Gaussian process regression with GPy. (A) Estimated yield from Table 2 (entries 1–5); (B) Predicted yield for flow rates in the yellow ring in Fig. 2A; (C) Predicted yield for temperatures in the yellow ring in Fig. 2A; (D) Estimated yield from Table 2 (entries 6–10); (E) Predicted yield for equivalents of **2a** in the yellow ring in Fig. 2D; (F) Predicted yield for temperatures in the yellow ring in Fig. 2D.

Scheme 1. Scope of RC and [3+2] annulation sequence.

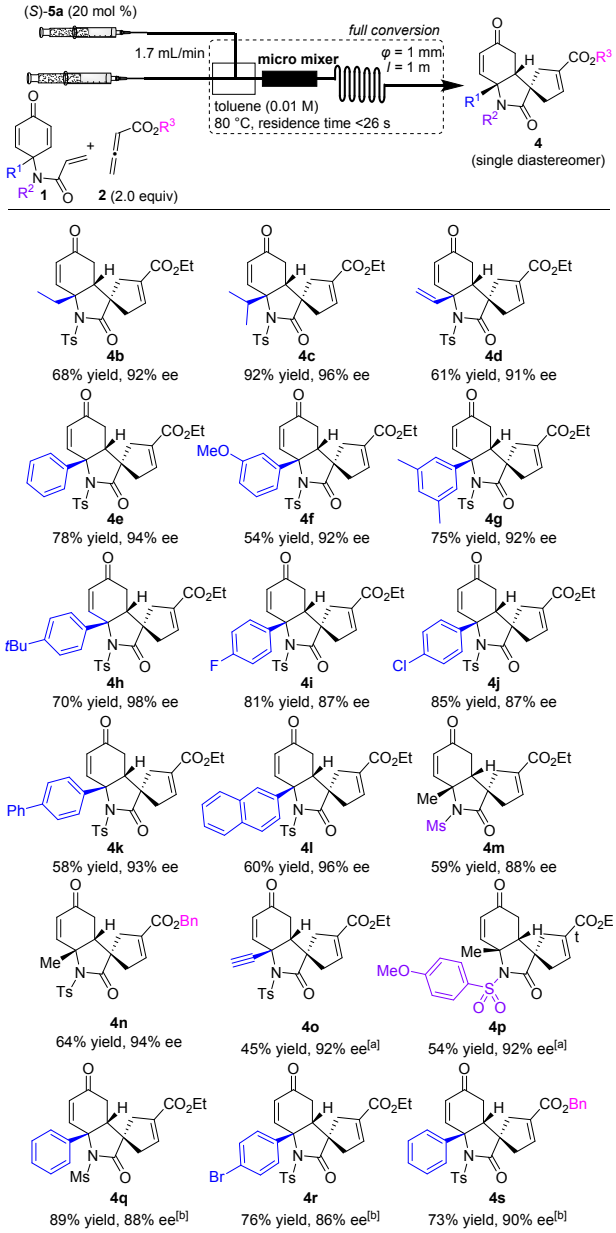

Yields are those of isolated **4**. The ee value of **4** was determined by HPLC analysis (Daicel Chiralpak ID for **4b-4e**, **4g**, **4h**, **4k** and **4p**; Daicel Chiralpak IC for **4f**, **4i**, **4j**, **4n**, **4r** and **4s**; Daicel Chiralpak IB for **4m** and **4q**; and Daicel Chiralpak IE for **4l** and **4o**). Reaction conditions: **1** (0.03 mmol), **2** (2.0 equiv.), and catalyst (*S*)-**5a** (20 mol%) in degassed dry toluene (3 mL), micro mixer: Comet X-01, stainless-steel tube: internal diameter: 1.0 mm; length: 1.0 m, flow rate: 1.7 mL/min, residence time: 26 s, at 80 °C. [a]1.5 equiv. of **2a**. [b]Residence time: 21 s (flow rate: 2.1 mL/min).

4b (68% yield, 92% ee) and **4c** (92% yield, 96% ee). Similarly, starting material **1d** bearing a vinyl group provided the corresponding spirocyclic compound **4d** in 61% yield and 91% ee. Dienones **1e–l** bearing an electron-donating or electron-withdrawing substituent on the aryl group reacted with allenoate **2a** to give the corresponding products **4e–l** (54–85% yield, 87–98% ee). Additionally, the acrylic amide containing a methanesulfonyl group as the R^2 group (**1m**) yielded spiro heterocycle **4m** with moderate success (59% yield, 88% ee). The reaction of dienone **1a** with benzyl allenoate **2b** could be achieved to give product **4n** in 64% yield and 94% ee. The reaction of **1o** (R^1 = ethynyl, R^2 = tosyl) and **1p** (R^1 = methyl, R^2 = 4-methoxyphenyl sulfonyl) with **2a** (1.5 equiv.) provided desired products **4o** (45% yield, 92% ee) and **4p** (54% yield, 92% ee). The chiral spirocycles **4q** and **4r** were obtained within 21 s residence time in 89% yield and 88% ee, and 76% yield and 86% ee, respectively (flow rate: 1.5 mL/min). Similarly, dienone **1e** and benzyl allenoate **2b** were also converted into the corresponding product **4s** in 73% yield and 90% ee under the same conditions as for **4q** and **4r**. The absolute configuration of chiral spiro compound **4e** with catalyst (*S*)-**5a** was determined to be *S,R,R* by single X-ray crystallographic analysis (see Supplementary Fig. S6).

A plausible reaction mechanism for this sequential reaction is shown in Fig. 3. Under the dilute concentration of substrates, initially, the intramolecular RC reaction proceeds as: The addition of catalyst **5a** to the acrylamide terminal on **1a** generates **Intermediate A** (**Int. A**). The chiral enolate in **Int. A**. subsequently reacts with one of the olefins on the dienone unit to generate **Int. B**. Then, deprotonation of α-proton of the carbonyl group in **Int. B** affords **Int. C** (**3a**) bearing a highly reactive exo-olefin, which is subsequently trapped with allenoate **2a** via [3+2] annulation. In the intermolecular [3+2] annulation supported by the micro-mixing flow system, allenoate **2a** reacts with regenerated organocatalyst **5a** to afford **Int. D**, resulting in Michael reaction of the exo-olefin in **Int. C**, despite the dilute concentration of the reactants (significantly important, to suppress side reactions in the presence of many highly reactive species as shown in Fig. 3). Next, the electron deficient phosphonium cation in **Int. E** prompts the conjugate addition of enolate to give **Int. F**. Finally, the desired product **4a** is formed through proton-transfer and elimination of catalyst from **Int. F**.

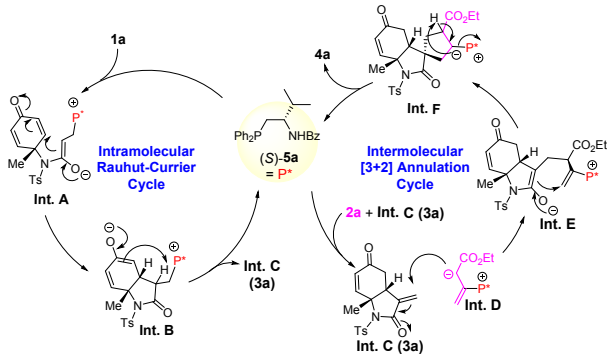

Fig. 3 Proposed reaction mechanism.

We demonstrated the highly atom-economical chemo-, regio-, enantio-, and diastereoselective domino reaction initiated by RC and [3+2] annulation sequence using an organocatalyst in a flow system. GPR was successfully applied to multi-parameter reaction screening. The present domino reaction provided chiral spiro heterocycles with three contiguous chiral centers in excellent results within one minute under the optimal conditions. This helpful exploration methodology of suitable reaction conditions will be applicable to other time-consuming reaction optimizations. Further practical applications of GPR for other reaction optimization as well as the use of an immobilized catalyst are also under way in our laboratory.

Conflicts of interest

There are no conflicts of interest to declare.

Notes and references

1. (*a*) J. Bergstra, R. Badenet, Y. Bengio and B. Kégl, *NIPS,* 2011, **24**, 2546−2554; (*b*) J. Bergstra and Y. Bengio, *J. Mach. Learn. Res.,* 2012, **13**, 281−305; (*c*) T. Back, Evolutionary algorithms in theory

and practice: Evolution strategies, evolutionary programming, genetic algorithms, Oxford University Press, New York, 1996.

2. (*a*) G. Schneider, *Nat. Rev. Drug Discov.,* 2018, **17**, 97–113; (*b*) H. Chen, O. Engkvist, Y. Wang, M. Olivecrona and T. Blaschke, *Drug Discov. Today*, 2018, **23**, 1241–1250; (c) X. Yang, Y. Wang, R. Byrne, G. Schneider and S. Yang, *Chem. Rev.*, 2019, **119**, 10520-10594.
3. (*a*) S. Szymkuć, E. P. Gajewska, T. Klucznik, K. Molga, P. Dittwald, M. Startek, M. Bajczyk and B. A. Grzybowski, *Angew. Chem., Int. Ed.,* 2016, **55**, 5904−5937; (*b*) J. N. Wei, D. Duvenaud and A. Aspuru-Guzik, *ACS Cent. Sci.,* 2016, **2**, 725−732; (*c*) C. W. Coley, R. Barzilay, T. S. Jaakkola, W. H. Green and K. F. Jensen, *ACS Cent. Sci.,* 2017, **3**, 434−443; (*d*) M. H. S. Segler, M. Preuss and M. P. Waller, *Nature,* 2018, **555**, 604–610; (*e*) C. W. Coley, W. H. Green and K. F. Jensen, *Acc. Chem. Res.,* 2018, **51**, 1281–1289; (*f*) O. Engkvist, P.-O. Norrby, N. Selmi, Y.-H. Lam, Z. Peng, E. C. Sherer, W. Amberg, T. Erhard and L. A. Smyth, *Drug Discov. Today,* 2018, **23**, 1203−1218; (*g*) A. F. de Almeida, R. Moreira and T. Rodrigues, *Nat. Rev. Chem.*, 2019, **3**, 589–604; (*h*) J. S. Schreck, C. W. Coley and K. J. M. Bishop, *ACS Cent. Sci.,* 2019, **5**, 970–981.
4. (*a*) P. Raccuglia, K. C. Elbert, P. D. F. Adler, C. Falk, M. B. Wenny, A. Mollo, M. Zeller, S. A. Friedler, J. Schrier and A. J. Norquist, *Nature,* 2016, **533**, 73–76. (*b*) M. S. Sigman, K. C. Harper, E. N. Bess and A. Millo, *Acc. Chem. Res.,* 2016, **49**, 1292–1301. (*c*) B. Sanchez-Lengeling and A. Aspuru-Guzik, *Science,* 2018, **361**, 360–365. (*d*) K. T. Butler, D. W. Davies, H. Cartwright, O. Isayev and A. Walsh, *Nature,* 2018, **559**, 547–555. (*e*) A. F. Zahrt, J. J. Henle, B. T. Rose, Y. Wang, W. T. Darrow and S. E. Denmark, *Science*, 2019, **363**, eaau5631. (*f*) D. J. Durand and N. Fey, *Chem. Rev.,* 2019, **119**, 6561–6594.
5. (*a*) B. J. Reizman and K. F. Jensen, *Acc. Chem. Res.,* 2016, **49**, 1786−1796. (*b*) V. Sans and L. Cronin, *Chem. Soc. Rev.,* 2016, **45**, 2032–2043. (*c*) D. E. Fitzpatrick, T. Maujean, A. C. Evans and S. V. Ley, *Angew. Chem., Int. Ed*., 2018, **57**, 15128–15132. (*d*) A.-C. Bédard, A. Adamo, K. C. Aroh, M. G. Russell, A. A. Bedermann, J. Torosian, B. Yue, K. F. Jensen and T. F. Jamison, *Science,* 2018, **361**, 1220–1225. (*e*) M. Trobe and M. D. Burke, *Angew. Chem., Int. Ed.,* 2018, **57**, 4192–4214.
6. (*a*) Z. Zhou, X. Li and R. N. Zare, *ACS Cent. Sci.,* 2017, **3**, 1337−1344.
(*b*) H. Gao, T. J. Struble, C. W. Coley, Y. Wang, W. H. Green and K. F. Jensen, *ACS Cent. Sci.,* 2018, **4**, 1465-1476. (*c*) L. Ḧase, L. M. Roch, C. Kreisbeck and A. Aspuru-Guzik, *ACS Cent. Sci.,* 2018, **4**, 1134–1145. (*d*) A. M. Schweidtmann, A. D. Clayton, N. Holmes, E. Bradford, R. A. Bourne and A. Lapkin, *Chem. Eng. J.,* 2018, **352**, 277−282. (*e*) P. Vámosi, K. Matsuo, T. Masuda, K. Sato, T. Narumi, K. Takeda and N. Mase, *Chem. Rec.,* 2019, **19**, 77–84.
7. For selected recent reports on GPR for theoritical- and physical chemistry, see: (*a*) C. E. Rasmussen and C. K. Williams, Gaussian processes for machine learning; MIT Press: Cambridge, MA, USA, 2006; Vol. 1. (*b*) J. P. Aborzpour, D. P. Tew and S. Habershon, *J. Chem. Phys.,* 2016, **145**, 174112. (*c*) O.-P. Koistinen, F. B. Dagbjartsdóttir, V. Ásgeirsson, A. Vehtari and H. Jónsson, *J. Chem. Phys.,* 2017, **147**, 152720. (*d*) R. Ramakrishnan and O. A. von Lilienfeld, Reviews in computational chemistry, Vol. 30; John Wiley & Sons, 2017; pp 225−256. (*e*) A. Denzel and J. Kästner, *J. Chem. Theory Comput.,* 2018, **14**, 5777–5786. (*f*) G. Schmitz and O. Christiansen, *J. Chem. Phys*., 2018, **148**, 241704; (*g*) G. Schmitz, D. G. Artiukhin and O. Christiansen, *J. Chem. Phys.*, 2019, **150**, 131102.
8. (*a*) C. V. Calliford and K. A. Scheidt, *Angew. Chem., Int. Ed.,* 2007, **46**, 8748−8758; (*b*) R. Narayan, M. Potowski, Z.-J. Jia, A. P. Antonchick and H. Waldmann, *Acc. Chem. Res.,* 2014, **47**, 1296−1310; (*c*) T. L. Pavlovska, R. G. Redkin, V. V. Lipson and D. V. Atamanuk, *Mol. Diversity,* 2016, **20**, 299–344; (*d*) B. Yu, D.-Q. Yu and H. M. Liu, *Eur. J. Med. Chem.,* 2015, **97**, 673−698; (*e*) N. Ye, H. Chen, E. A. Wold, P.-Y. Shi and J. Zhou, *ACS Infect. Dis.,* 2016, **2**, 382–392; (*f*) S. S. Panda, R. A. Jones, P. Bachawala and P. P. Mohapatra, *Mini-Rev. Med. Chem.,* 2017, **17**, 1515–1536.
9. For selected recent reviews and reports on asymmetric synthesis of spirooxindoles, see: (*a*) G.-J. Mei and F. Shi, *Chem. Commun.,* 2018, **54**, 6607–6621; (*b*) S. Takizawa, K. Kishi, M. Kusaba, B. Jianfei, T. Suzuki and H. Sasai, *Heterocycles,* 2017, **95**, 761–767; (*c*) W. He, J. Hu, P. Wang, L. Chen, K. Ji, S. Yang, Y. Li, Z. Xie and W. Xie, *Angew. Chem., Int. Ed.,* 2018, **57**, 3806–3809; (*d*) T. Kang, P. Zhao, J. Yang, L. Lin, X. Feng and X. Liu, *Chem. Eur. J.,* 2018, **24**, 3703–3706.
10. Our recent reports on domino reaction, see: (*a*) S. Takizawa, K. Kishi, Y. Yoshida, S. Mader, F. A. Arteaga, S. Lee, M. Hoshino, M. Rueping, M. Fujita and H. Sasai, *Angew. Chem., Int. Ed.,* 2015, **54**, 15511–15515; (*b*) M. Sako, Y. Takeuchi, T. Tsujihara, J. Kodera, T. Kawano, S. Takizawa and H. Sasai, *J. Am. Chem. Soc.,* 2016, **138**, 11481–11484; (*c*) K. Kishi, F. A. Arteaga, S. Takizawa and H. Sasai, *Chem. Commun.,* 2017, **53**, 7724–7727; (*d*) K. Kishi, S. Takizawa and H. Sasai, *ACS Catal.,* 2018, **8**, 5228–5232.
11. For selected reviews and reports on enantioselective organocatalyzed domino reactions, see: (*a*) C. Zhang and X. Lu. *J. Org. Chem.,* 1995, **60**, 2906–2908; (*b*) *Domino reactions: Concepts for efficient organic synthesis* (Ed.: Tietze, L. F.), Wiley-VCH, Weinheim, 2014; (*c*) P. Chauhan, S. Mahajan and D. Enders, *Acc. Chem. Res*., 2017, **50**, 2809–2821; (*d*) H. Jin, Q. Zhang, E. Li, P. Jia, N. Li and Y. Huang, *Org. Biomol. Chem.,* 2017, **15**, 7097–7101; (*e*) X.-Y. Chen, S. Li, F. Vetica, M. Kumar and D. Enders, *iScience,* 2018, **2**, 1–26; (*f*) X. Wu, L. Zhou, R. Maiti, C. Mou, L. Pan and Y. R. Chi, *Angew. Chem., Int. Ed.,* 2019, **58**, 477–481; (*g*) H. Wang, J. Zhang, Y. Tu and J. Zhang, *Angew. Chem., Int. Ed.,* 2019, **58**, 5422–5426; (*h*) K. Li, T. P. Gonçalves, K.-W. Huang and Y. Lu, *Angew. Chem., Int. Ed.,* 2019, **58**, 5427–5431.
12. For selected publications on flow reactions, see: (*a*) J. Wegner, S. Ceylan and A. Kirschning, *Adv. Synth. Catal.,* 2012, **354**, 17–57; (*b*) I. R. Baxendale, *J. Chem. Technol. Biotechnol.,* 2013, **88**, 519–552; (*c*) J. C. Pastre, D. L. Browne and S. V. Ley, *Chem. Soc. Rev.,* 2013, **42**, 8849–8869; (*d*) T. Tsubogo, T. Ishiwata and S. Kobayashi, *Angew. Chem., Int. Ed.,* 2013, **52**, 6590–6604; (*e*) A. A. Folguerias-Amador and T. Wirth, *J. Flow Chem.,* 2017, **7**, 94–95; (*f*) J. Britton and C. L. Raston, *Chem. Soc. Rev.,* 2017, **46**, 1250–1271; (*g*) M. B. Plutschack, B. Pieber, K. Gilmore and P. H. Seeberger, *Chem. Rev.,* 2017, **117**, 11796–11893; (*h*) R. Gérardy, N. Emmanuel, T. Toupy, V.-E. Kassin, N. N. Tshibalonza, M. Schmitz and J.-C. M. Monbaliu, *Eur. J. Org. Chem.,* 2018, 2301–2351; (*i*) S. Santoro, F. Ferlin, L. Ackermann and L. Vaccaro, *Chem. Soc. Rev.*, 2019, **48**, 2767–2782. (j) D. Perera, J. W. Tucker, S. Brahmbhatt, C. J. Helal, A. Chong, W. Farrell, P. Richardson, N. W. Sach, *Science*, 2019, **359**, 429-434. (k) C. W. Coley, D. A. Thomas III, J. A. M. Lummiss, J. N. Jaworski, C. P. Breen, V. Schultz, T. Hart, J. S. Fishman, L, Rogers, H. Gao, R. W. Hicklin, P. P. Plehiers, J. Byington, J. S. Piotti, W. H. Green, A. J. Hart, T. F. Jamison, K. F. Jensen, *Science*, DOI: 10.1126/science.aax1566.
13. A micromixing device, 'Comet X-01', is available from Techno Applications Co., Ltd., 34-16-204, Hon, Denenchofu, Oota, Tokyo, 145-0072, Japan.
14. RC reaction of dienone **1a**, followed by introduction of allenoate **2a** in flow system decreased yield of product **4a**.
15. The GPy authors. GPy: A Gaussian process framework in python. http://github.com/ SheffieldML/Gpy.
16. Although three parameters (flow rate, temperature, and equivalent of **2a**) can be calculated simultaneously through GPR, more experimental data (at least 30 as minimum number of data) are required to accurately predict optimal conditions. Therefore, the suitable reaction condition was estimated from temperature and flow rate, then temperature and equivalent of **2a**, followed by flow rate and quantity of **2a**.
17. This result was also supported by predicted yield from flow rate, and quantity of **2a** at 80 °C with GPy (see Supplementary Table S5 and Fig. S5).

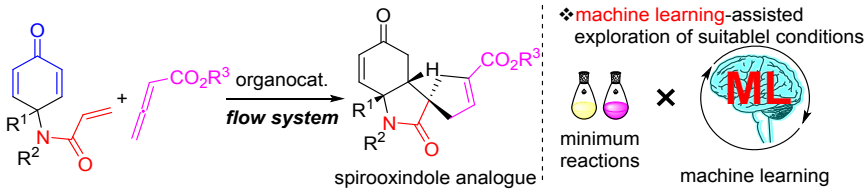

A highly atom-economical enantioselective Rauhut-Currier and [3+2] annulation has been established by flow system and machine-learning-assisted exploration of suitable conditions.